Supporting Information

S1. The structural analysis of tetragonal rutile VO_2, monoclinic VO_2, and orthorhombic paramontroseite VO_2.

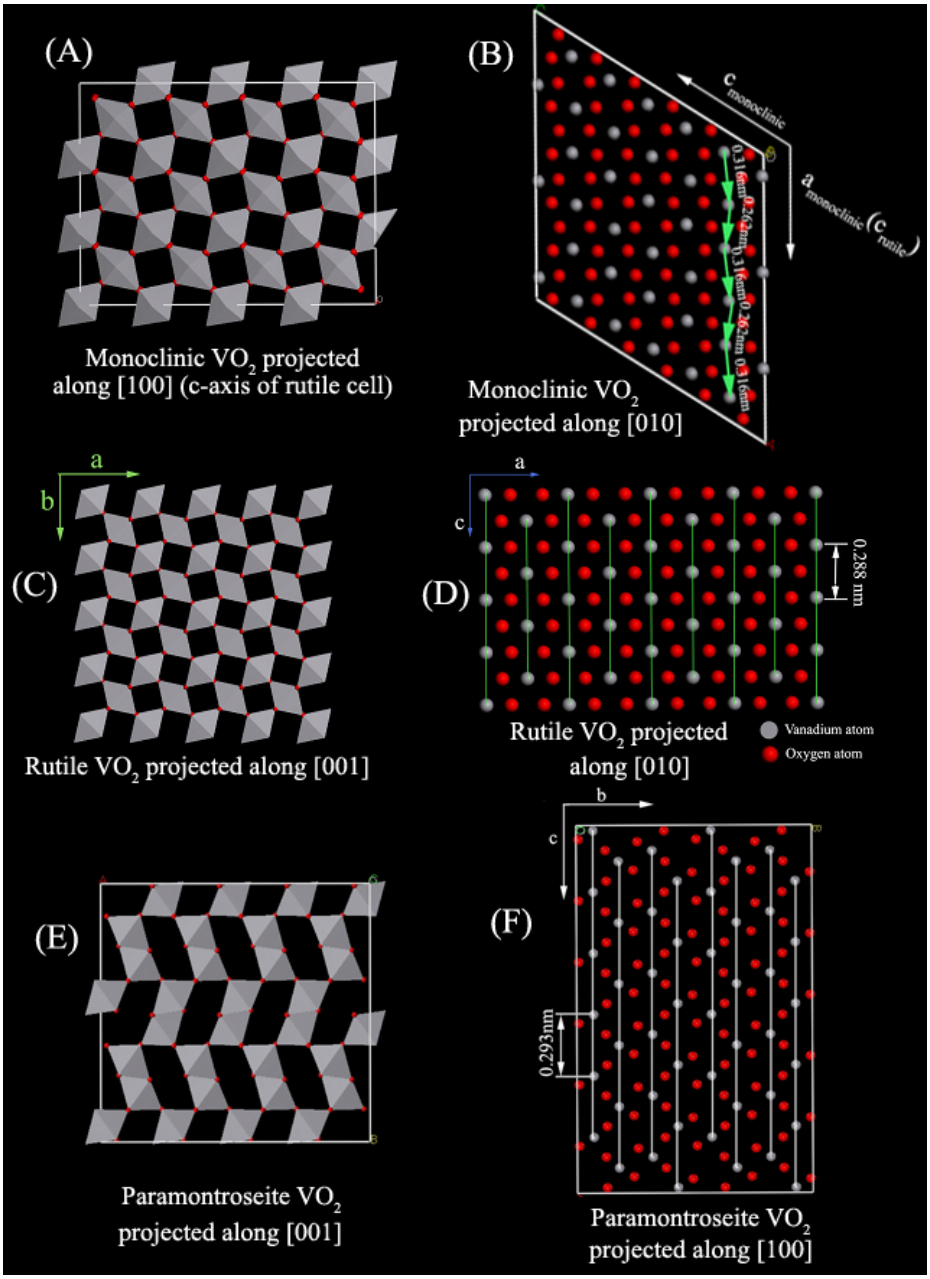

Figure S1. (A) Crystal structure of monoclinic VO_2 projected along [100] (c-axis of rutile cell). (B) The super-cell structure of monoclinic VO_2 projected along [010]. The distortion of vanadium atom could be clearly seen by the green color arrows along the a-axis (c-axis of rutile cell). (C) Crystal structure of tetragonal rutile VO_2 projected along [001]; (D) The super-cell structure of rutile VO_2 projected along [010], and vanadium atoms built chains parallel to the c axis of the structure. (E) The super-cell structure of orthorhombic paramontroseite VO_2 projected along [001]; (F) The super-cell structure of orthorhombic paramontroseite VO_2 projected along [100] and

the vanadium atoms built chains parallel to the c axis of the structure, and vanadium atoms built chains parallel to the c axis of the paramontroseite structure.

Both the tetragonal rutile and monoclinic VO_2 are based on a given oxygen bcc lattice and the different positions of vanadium ions (V^{4+}) determine the different crystal phase kind. In tetragonal rutile VO_2 crystal structure, the nearest V-V distance between the neighboring V atoms is 0.288 nm and the vanadium atoms form the infinite chains along the rutile c-axis (c_R-axis), which makes the d-orbit electrons shared by all of the metal V atoms along this direction, leading to its metallic behavior (**Figure S1C-D**). Meanwhile, the monoclinic VO_2 has two different V-V distances of 0.262 and 0.316 nm between the nearest vanadium atoms, forming zigzag-type vanadium atoms along the c_R-axis, which have shifted from the center of the octahedral and form chains that are no longer parallel to the c_R-axis. (**Figure S1E-F**) Thus, the d-orbit electrons are localized in these vanadium atoms with zigzag-type direction, resulting in the insulator behavior of monoclinic VO_2. In a word, the small structural distortion of VO_2 lattice would lead to the different electrical properties of VO_2, which inspire us to further pursue the fascinatingly physical and chemical properties for other functional vanadium oxides.

S2. The introduction of VASP programe and the spin-dependent energy bands of the paramontroseite VO_2

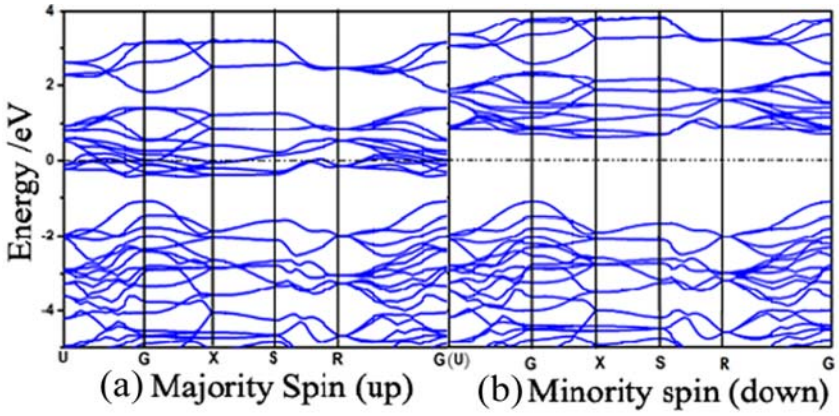

Figure S2 (c-d) Spin-dependent energy bands of the paramontroseite VO_2: (a) Majority spin (up); (b) Minority spin (down).

The Vienna Ab Initio Simulation Package (VASP) is the leading first-principles method for computing materials properties based on electronic structure, yielding the electrical properties such as electronic band structure and density of states, etc. Within the density functional formalism, VASP can be used to simulate a wide range of materials including crystalline solids, surfaces, molecules, liquids and amorphous materials, where the properties of any material that can be thought of as an assembly of nuclei and electrons are calculated with the only limitation being the finite speed and memory of the computers being used. Therefore, the theoretical calculations by VASP are considered to be a significant aid in predicting the electrical properties of materials, such as insulating, semiconducting, or conducting properties[1].

S3. Additional experimental details

Using the reducing effect of TAA[17], the whole reaction for the synthesis of paramontroseite VO_2 could be shown as follow:

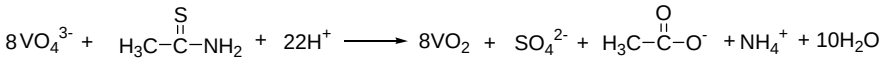

$$8VO_4^{3-} + H_3C-\overset{\overset{S}{\|}}{C}-NH_2 + 22H^+ \longrightarrow 8VO_2 + SO_4^{2-} + H_3C-\overset{\overset{O}{\|}}{C}-O^- + NH_4^+ + 10H_2O$$

VASP is a periodic DFT program using the projector augmented wave (PAW) method. [2] The geometric optimization process was carried out using a convergence of 2 meV for VASP. For the VASP calculations, convergence was attained with a $11\times11\times4$ Monkhorst-Pack [3] k-point grid and planewave and augmentation charge cutoffs of 780 and 400 eV.

The electrochemical performance of the VO_2 sample for aqueous LIBs was evaluated using a Teflon cell, where the excess $LiMn_2O_4$ was conducted in order to precisely evaluate the electrochemical capability of paramontroseite VO_2. The preparation of negative and positive electrodes was conducted in a similar way. The electrode was prepared by pressing the mixture of sample / acetylene black / poly (vinylidene fluoride) (PVDF) with weight ratio of 80/10/10. The electrolyte was the aqueous solution including 5M $LiNO_3$ and 0.001 M LiOH. The discharge and charge tests for aqueous LIBs were carried out using the Land battery system (CT2001A) at a constant current density with a cutoff voltage of 1.65 - 0.5 V.

S4. Morphology information of the as-obtained paramontroseite product

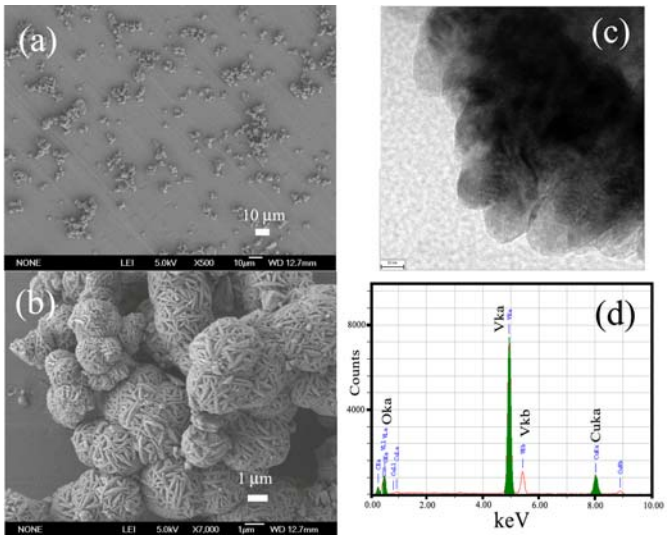

Figure S4. (a) The panoramic morphology of the as-obtained paramontroseite VO_2 product was revealed by the field emission scanning electron microscopy (FE-SEM). (b) The magnified FE-SEM image, where the numerous nanoflakes are aligned perpendicularly to the surface of spheres with a puffy appearance, showing the walnut-like morphology. (c) Typical TEM image of a typical walnut-like particle. (d) The energy-disperse X-ray (EDX) pattern for VO_2 walnut-like architectures. The EDX spectroscopic analysis (**Figure S4d**) of the walnut-like nanoarchitecture shows that there is only V and O elements can be observed from the walnut-like nanoarchitectures, while the Cu signal arises from the TEM grid. However, the atom

ratio of V and O cannot be determined because one peak for the element V overlaps with that for the element O.

S5. SAED pattern analysis

The angle values between the lattice planes which appeared in the SAED patterns provides a further evidence for the paramontroseite VO_2 synthesized in our reaction systems. The experimental angle value could be achieved by directly measuring the corresponding angle between the two lines, where the lines were formed by the link of each of two points (representing the concerned two lattice planes) and its zone-axis point in the SAED pattern, respectively. While the theoretical angle value were obtained by the calculation based on the orthorhombic crystallographic parameters of paramontroseite VO_2. The relevant formula could be shown as follows:

$$Lattice\ Plane\ Angle = \frac{\frac{h_1 \times h_2}{a \times a} + \frac{k_1 \times k_2}{b \times b} + \frac{l_1 \times l_2}{c \times c}}{\sqrt{((\frac{h_1 \times h_1}{a \times a} + \frac{k_1 \times k_1}{b \times b} + \frac{l_1 \times l_1}{c \times c}) \times (\frac{h_2 \times h_2}{a \times a} + \frac{k_2 \times k_2}{b \times b} + \frac{l_2 \times l_2}{c \times c}))}}$$

All the results are summarized in **Table S5-1**, from which one can find that the experimental angle values agree well with the corresponding theoretical ones, giving the evidence that the as-obtained vanadium dioxides was orthorhombic paramontroseite VO_2.

Another important evidence for the presence of paramontroseite comes from the comparison of the theoretically calculated pattern in the previous report [4] and our SAED pattern for paramontroseite. **Figure S5-1** shows the calculated and our experimental diffraction pattern along b axis, from which one can find that the high similarity between these two SAED patterns, further confirming that the as-obtained product was paramontroseite VO_2 from the microscopic structural point of view. Therefore, the consistence of these two SAED patterns provides a solid evidence for the presence of paramontroseite VO_2, which could be obtained from the simple hydrothermal process.

Table S5. The summary information of the experimental angle values, and the theoretical angle values for the as-obtained paramontroseite VO_2.

Lattice Plane		Theoretical Angle Value	Experimental Angle Value
(101)	(200)	59.26 °	59.5 °
	(301)	29.98 °	29.9 °
	(002)	30.73 °	30.5 °
	(020)	90.00 °	90.0 °
	(121)	28.01 °	28.1 °
	(240)	69.27 °	69.4 °
(200)	(301)	29.28 °	29.4 °
(121)	(020)	61.98 °	60.8 °
(200)	(002)	90.00 °	90.0 °

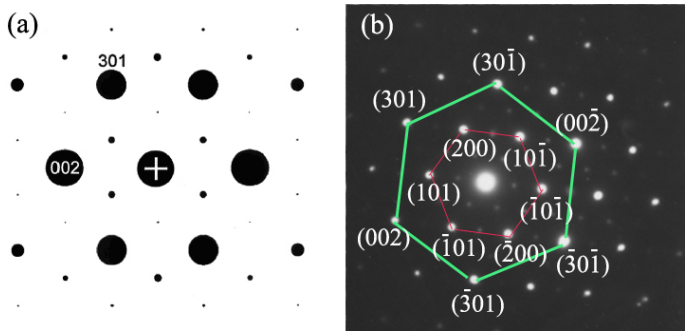

Figure S5 (a) Calculated diffraction pattern of paramontroseite along b axis in the reported literature [L. Löffler, W. Mader, *J. Am. Ceram. Soc.* 2003, **86**, 534.] (b) The experimental diffraction pattern along b axis performed on the edge of one typical paramontroseite VO_2 walnut-like architectures. The consistence of these two SAED patterns provides a solid evidence for the presence of paramontroseite VO_2.

S6. Additional characterization for the chemical composition of as-obtained product

Important information about the surface molecular and electronic structure of the as-obtained vanadium-including products, as well as the valence of vanadium ion can be provided by the X-ray photoelectron spectroscopy (XPS) as shown in **Figure S6a**. X-ray photoelectron spectroscopy (XPS) measurements were performed on a VGESCALAB MKII X-ray photoelectron spectrometer with an exciting source of Mg K□= 1253.6 eV. The binding energies obtained in the XPS analysis were corrected for specimen charging by referencing the C_{1s} to 284.60 eV. The O_{1s} binding energy (top inset in **Figure S6a**, 529.6 eV) indicates that the oxygen atoms exist as O^{2-} species in the compounds[5]. The V_{2p} core level spectrum (top inset in **Figure S6a**) illustrates that the observed value of the binding energies for $V_{2p3/2}$ and $V_{2p1/2}$ is in agreement with the literature values of bulk V^{4+} materials [6]. Additionally, it has established that the oxidation state of the vanadium oxides can be determined by the difference in binding energy (Δ) between the O_{1s} and $V_{2p3/2}$ level [7]. As for the as-obtained vanadium oxides in the present work, the Δ ($V_{2p3/2}$-O_{1s}) value was 13.9 eV, which was well consistent with the reported value of V^{4+} compounds in the literature [8], further confirming the vanadium valence to be +4. Besides, the S_{2p} satellite peaks characterizing S^{2-}, which are usually centered at about 160 ~ 162 eV [9], are not found in **Figure S6a**, indicating that there are no residual S impurity in the sample and showing the high purity of the as-obtained products. Moreover, the average atomic

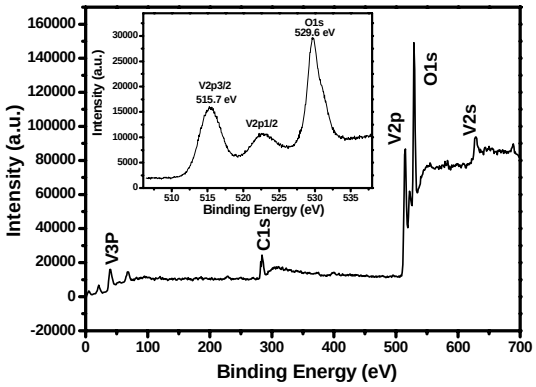

Figure S6. Survey XPS spectra of the as-obtained vanadium oxides product, and the top inset is the high resolution XPS for V_{2p} and O_{1s} region.

ratio of V and O is about 1: 2.01 on the basis of the quantification of V_{2p} and O_{1s} peaks.

References in the supporting information

[1] Y. H. Kim, S. S. Jang, Y. H. Jang, and W. A. Goddard III, Phys. Rev. Lett. 94, 156801, 2005

[2] (a) P. E. Blöchl, *Phys. Rev. B* 1994, **50**, 17953. (b) G. Kresse, J. Joubert, *Phys. Rev. B* 1999, **59**, 1758. (c) P. E. Blöchl, C. J. Först, J. Schimpl, *Bull. Mater. Sci.* 2003, **26**, 33.

[3] H.J. Monkhorst, J.D. Pack, *Phys. Rev. B* 1976, **13**, 5188.

[4] L. Löffler, W. Mader, *J. Am. Ceram. Soc.* 2003, **86**, 534.

[5] C. D. Wanger, W. M. Riggs, L. E. Davis, J. F. Moulder, G. E. Muilenberg, Handbook of X-ray Photoelectron Spectroscopy, Perkin-Elmer, Eden Prairie, (1978).

[6] G.A. Sawatzki and D. Post, *Phys. Rev. B.* 1979, **20**, 1546.

[7] J. Mendialdua, R. Casanova, Y. Barbaux, *J. Electron. Spectrosc. Relat. Phenom.* 1995, **71**, 249

[8] C. Blauw, F. Lechnhouts, F. Van der Woude, G.A. Sawatzki, *J. Phys. C.* 1975, **8**, 459.

[9] Z.Y. Meng, Y.Y. Peng, W.C. Yu, Y.T. Qian, *Mater. Chem. Phys.* 2002, **74**, 230.